BRCA1 Interaction with Non-Canonical DNA Structures: Insights into Genome Maintenance and Disease Mechanisms

Abstract

Breast Cancer Susceptibility Gene 1 (*BRCA1*) plays a crucial role in the homologous recombination (HR) pathway to repair double-stranded breaks (DSBs) in human cells. Interactions between BRCA1 protein and DNA have been mapped to the central region, which could be further divided as two DNA binding domains (DBDs); however, the relative substrate preferences of the DBDs and their functional role in HR remain poorly understood. We hypothesize that the DBDs have distinct binding preferences for DNA repair intermediates, and we have measured the DNA binding affinities of DBD1 (amino acids (aa) 330-554), DBD2 (aa894-1057), and the BRCA1 C-terminal repeats (BRCT) for single-stranded (ssDNA), double-stranded (dsDNA), and G-quadruplex (G4) DNA using biolayer interferometry. Our results indicate that DBD1 has the highest affinity for dsDNA, while DBD2 and BRCT bound tightest to G4 and ssDNA. Based on these findings, we propose a model in which DBD1 targets BRCA1 to DSBs for the promotion of DNA end resection, whereas DBD2 and BRCT target BRCA1 to telomeres to function in chromatin remodeling and telomere regulation.

Introduction

Breast Cancer Susceptibility Gene 1 (*BRCA1*) encodes a tumor suppressor protein that is critical for genome integrity maintenance, specifically through double-stranded break (DSB) repair, transcription regulation, and telomere maintenance [1, 2, 3, 4]. Mutations in *BRCA1* are linked to breast and ovarian cancer and certain cardiovascular diseases [5, 6]. BRCA1 coordinates DSB repair via homologous recombination (HR) by recruiting end-resection proteins such as 53BP1 [3, 7, 8]. This is subsequently followed by BRCA1 interaction with PALB2 to recruit BRCA2/RAD51 for strand invasion [9, 10, 11]. BRCA1 also stabilizes stalled replication forks and aids in the restart of replication [12, 13].

Replication fork stress arises from impediments to replication, such as DNA damage, common fragile sites, and non-canonical B form DNA [14]. Failure to manage stress can lead to replication fork collapse, causing DSBs [15]. DSBs, among the most damaging DNA lesions, must be efficiently repaired to prevent tumorigenesis [16, 17]. Repair mechanisms include HR, non-homologous end joining (NHEJ), alternative end joining, and single-strand annealing, with HR being the most precise method [18, 19, 20, 21].

Non-canonical DNA structures, present in all living organisms, must be remodeled during replication, transcription, and repair [22]. Studies show that BRCA1 has preference for branched, non-B form DNA structures, such as D-loop, cruciform, quadruplex, and replication fork DNA structures [23, 24, 25, 26]. Given its role in telomere regulation and satellite DNA binding, the ability of BRCA1 to bind non-canonical DNA structures is of considerable significance [2, 4, 27]. Moreover, BRCA1-deficient cells are highly sensitive to G-quadruplex (G4) stabilizers such as CX-5461, which block replication forks and induce strand gaps or breaks [28, 29].

Although BRCA1 is largely structurally undefined, two structured domains have been identified: a ring finger domain (RING) at the N-terminus and two tandem repeats (BRCT) at the C-terminus. The RING domain forms a heterodimer with BARD1, functioning as an E3 ubiquitin ligase [30, 31, 32]. BRCA1-BARD1 preferentially binds to D-loops and DNA bubbles and is essential for RAD51-mediated HR and replication fork restart at G4 sites [24, 33]. In contrast, the BRCT domain exists as a phosphoprotein binding motif and is homologous to domains found in other DNA repair proteins [34]. Fanconi anemia complementation group J (FANCJ) specifically binds BRCT in the ICL/DSB repair pathway and promotes replication fork restart at G4s [35, 36, 37, 38]. BRCT domains also bind supercoiled DNA, facilitate chromatin remodeling when BRCA1 is tethered to chromosomes via the GAL4 DNA binding domain, and are involved in detecting DNA breaks [39, 40, 41 ,42]. Additionally, the BRCA1 BRCT domain suppresses ribosomal R-loops through two mechanisms: facilitating dsRNA formation between rRNA and as-rRNA, and promoting RNA polymerase I-dependent transcription of as-rRNA [43].

The unstructured central domain of BRCA1, acting as a scaffold, binds DNA and retains preference for non-B form DNA structures [23, 26, 42, 44]. Two DNA binding domains (DBDs) can be identified within this region, at amino acids (aa) 330-554 (DBD1) and 894-1057 (DBD2) [40, 43, 45, 46, 47]. While a previous study estimated the binding affinity of the DBDs for branched DNA with a 3’ flap, their binding affinities need further quantification [23]. We aim to determine the binding affinities of DBD1, DBD2, and BRCT for different DNA repair intermediates and discuss the significance of these values to the role of BRCA1 in DNA repair processes.

Results

BRCA1 DBD1 (aa330-554), DBD2 (aa894-1057), and the BRCT domain (aa1646-1863) were expressed and purified (Figure 1) from *E. coli* as discussed in the Materials and Methods. Binding experiments were conducted for DBD1, DBD2, and BRCT with different DNA repair intermediates (Table 1): single-stranded DNA (Bioss60R, or ssDNA), blunt-end double-stranded DNA (Biods60R-Cy3, or dsDNA), and a G-quadruplex sequence (BioG4Telo, or G4 DNA). The single-stranded and double-stranded sequences represent common DNA intermediates in homologous recombination. The G4 sequence, present in human telomeric DNA, was studied due to its role in BRCA1-mediated restart of stalled replication forks [28, 29]. Branched-point DNA was not included in the study to ensure direct 1:1 binding interactions between protein and DNA.

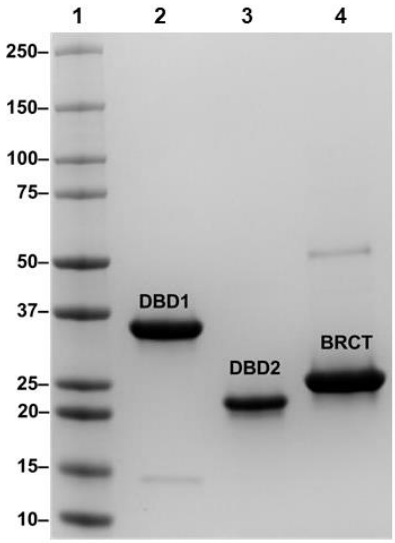

Figure 1. SDS-PAGE of purified recombinant proteins BRCA1 DBD1, DBD2, and BRCT. Lane 1 is a protein ladder with known molecular weights (kDa) that are labeled on the SDS-PAGE. Purified DBD1 was loaded in Lane 2. DBD1 was resolved as a homogeneous band at ~37 kDa. Purified DBD2 was loaded in Lane 3 and migrated as a ~22 kDa band. Purified BRCT was loaded in Lane 4. BRCT is observed at ~25 kDa.

Table 1. DNA oligo sequences

Name	**Sequence (5'→3')**	**Molar Extinction Coefficient ($M^{-1}cm^{-1}$)**	**Molecular Weight (g/mol)**
Bioss60R	/5Biosg/CCATGGCTCCTGAGCTAGCTGCAGTAGCCTAAAGGATGAAACTAGGATCTTATGCTCCAT	574,200	18,459.04
BioG4Telo	/5Biosg/TTAGGGTTAGGGTTAGGGTTAGGG	244,600	7,575
Cy3ss60RC	/5Cy3/ATGGAGCATAAGATCCTAGTTTCATCCTTTAGGCTACTGCAGCTAGCTCAGGAGCCATGG	582,700	18,996.6
Biods60R-Cy3	Bioss60R + Cy3ss60RC		37,849

Binding interactions between the proteins and various DNA repair intermediates were assessed using biolayer interferometry (BLI), a label-free method for measuring biomolecular interactions (Figure 2). The streptavidin (SA) tip was equilibrated with Buffer G, and biotinylated

DNA was loaded onto the tip, producing the initial optical interference. After loading, the tip was washed in Buffer G to establish a new baseline. Proteins were added to initiate the association, and after reaching binding equilibrium, the tip was placed into Buffer G for dissociation (Figure 2A). These studies were conducted at different protein concentrations. Figure 2B illustrates the association and dissociation steps at varying protein concentrations. At the end of the association step, the binding equilibrium plateau was plotted against protein concentration and fit to a 1:1 interaction model using non-linear least squares analysis to calculate equilibrium K values (Figure 2C).

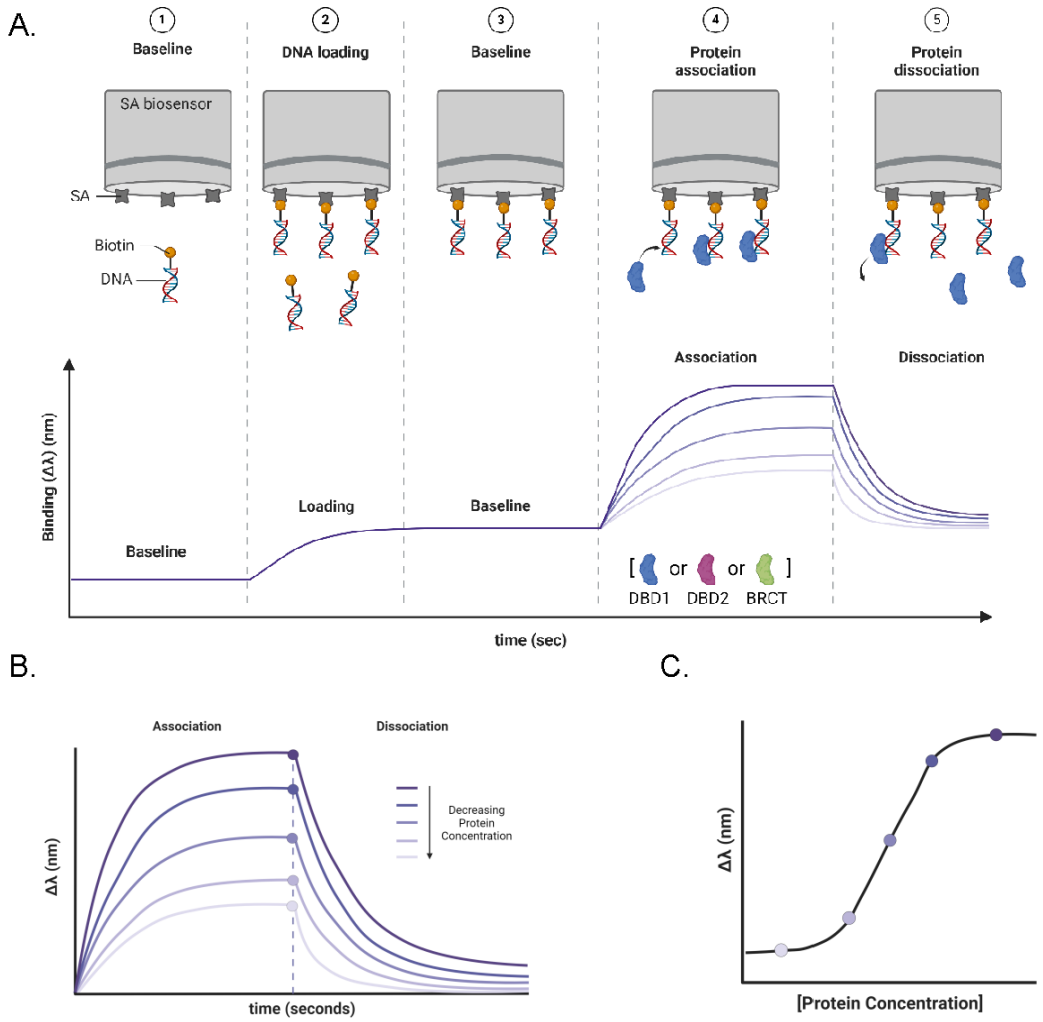

Figure 2. Biolayer interferometry (BLI) time-course and analysis. **A.** Cartoon depicting a time-course of the five steps of a BLI experiment. The interference pattern of a streptavidin-coated (SA) biosensor was measured in Buffer G to establish a baseline (Phase 1). Biotinylated DNA was loaded onto the sensor tip through biotin-SA interactions and an increase in Δλ was measured (Phase 2). The biosensor was washed with buffer to confirm the DNA substrate remained surface-

immobilized and to establish a new baseline (Phase 3). Protein (DBD1, blue; DBD2, magenta; BRCT, green) was introduced to initiate the association reaction (Phase 4). Once a binding equilibrium was reached, the biosensor was returned to Buffer G to examine the dissociation of the protein-DNA complexes (Phase 5).

DBD1 showed the highest affinity for dsDNA (K = 2.92 ± 0.66 x 10^7 M^{-1}) and the weakest for G4 DNA (K = 1.52 ± 0.28 x 10^7 M^{-1}) (Figure 3). DBD2 exhibited the opposite pattern, with the strongest binding to G4 DNA (K = 3.26 ± 1.27 x 10^7 M^{-1}) and the weakest to dsDNA (K = 2.27 ± 0.31 x 10^7 M^{-1}) (Figure 4). BRCT followed the same affinity pattern as DBD2, binding the strongest to G4 DNA (K = 6.82 ± 1.09 x 10^6 M^{-1}) and the weakest to dsDNA (K = 5.46 ± 0.42 x 10^6 M^{-1}) (Figure 5). Notably, BRCT had an order of magnitude lower binding affinity for each DNA compared to DBD2 (Table 2).

Figure 3. Plots of BRCA1 DBD1. **A.** ssDNA. **B.** dsDNA. **C.** G4 DNA.

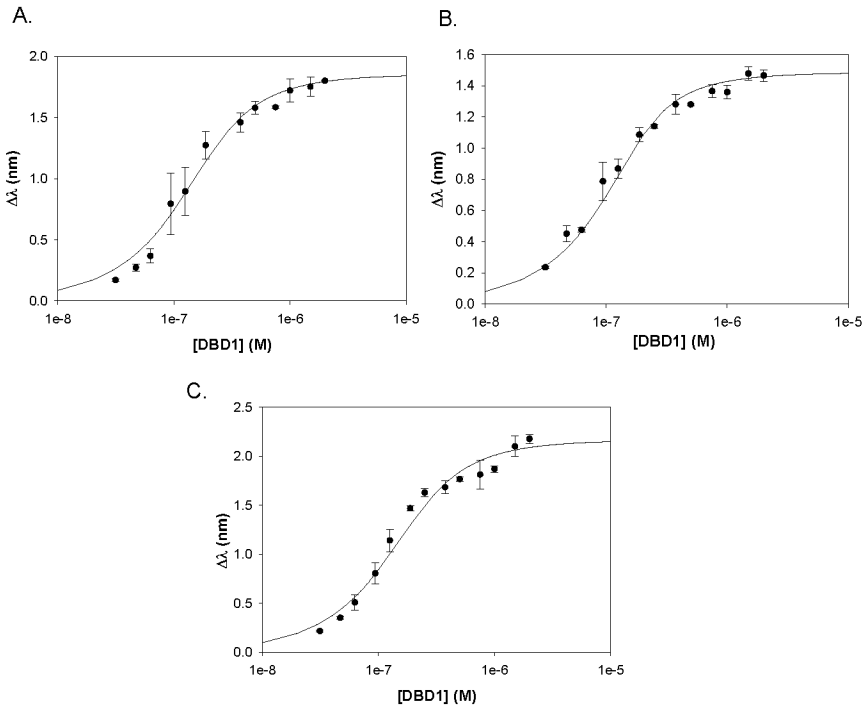

Figure 4. Plots of BRCA1 DBD2. **A.** ssDNA. **B.** dsDNA. **C.** G4 DNA.

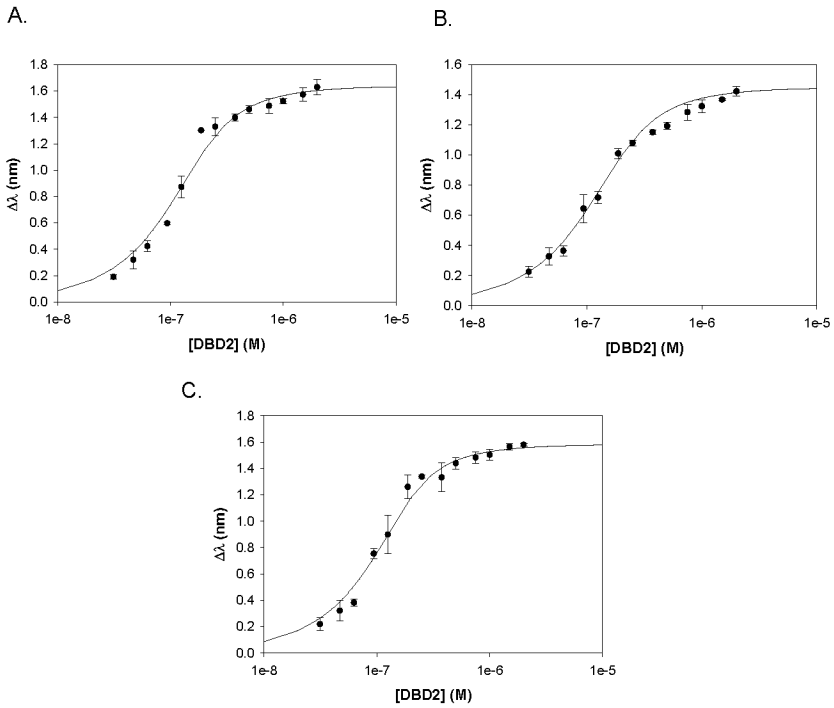

Figure 5. Plots of BRCA1 BRCT. **A**. ssDNA. **B.** dsDNA. **C.** G4 DNA.

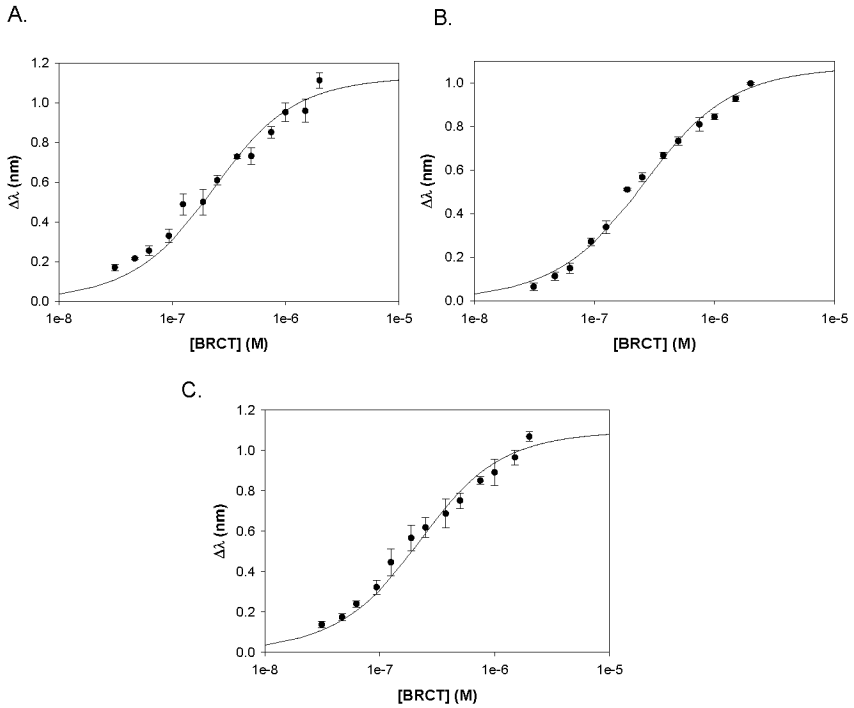

Table 2. Summary of BLI data

Protein	DNA Sequence	K (M^{-1})	A	R^2
DBD1	Bioss60R	$1.67 \pm 0.65 \times 10^7$	1.85 ± 0.037	0.995
	BioG4Telo	$1.52 \pm 0.28 \times 10^7$	2.16 ± 0.044	0.995
	Biods60R-Cy3	$2.92 \pm 0.66 \times 10^7$	1.48 ± 0.021	0.997
DBD2	Bioss60R	$2.47 \pm 0.23 \times 10^7$	1.64 ± 0.029	0.996
	BioG4Telo	$3.26 \pm 1.27 \times 10^7$	1.58 ± 0.023	0.997
	Biods60R-Cy3	$2.27 \pm 0.31 \times 10^7$	1.45 ± 0.043	0.996
BRCT	Bioss60R	$6.34 \pm 0.49 \times 10^6$	1.13 ± 0.027	0.993
	BioG4Telo	$6.82 \pm 1.09 \times 10^6$	1.09 ± 0.021	0.995
	Biods60R-Cy3	$5.46 \pm 0.42 \times 10^6$	1.07 ± 0.016	0.997

Discussion

The central DNA binding domain (DBD) of BRCA1, initially identified by Paull et al. as aa452-1079, shows a strong affinity for non-canonical DNA structures such as cruciform, supercoiled, quadruplex, and triplex DNA [23, 26, 46, 47]. Brázda et al. defined the DBD as aa444-1057 [26], while Masuda et al. reported it as aa421-701 [25]. Mark et al. identified two domains within the DBD, spanning aa498-663 and aa936-1057 [44]. Similarly, Naseem et al. isolated the first DBD domain to aa340-554 [48], while Brázda et al. isolated the second domain to aa894-1057 [47]. Based on these studies, we generated BRCA1 constructs DBD1 (aa330-554) and DBD2 (aa894-1057). The BRCT domain, known to interact with DNA and proteins involved in DNA repair and recombination [49], was also studied using a BRCT construct (aa1646-1863). Previous studies, while informative, used qualitative methods that did not provide exact DNA binding affinities. It is also unclear whether these BRCA1 domains function independently or depend on each other for full efficiency. We assessed the DNA binding affinities of BRCA1 constructs DBD1, DBD2, and BRCT for three DNA intermediates. DBD1 showed the highest affinity for dsDNA, followed by ssDNA, and the lowest affinity for G4 DNA. DBD2 and BRCT bound tightest to G4 DNA, followed by ssDNA, and bound weakest to dsDNA.

Our data fits a 1:1 interaction model, indicating that BRCA1 binds DNA with a 1-to-1 stoichiometry. The preference of DBD1 for dsDNA suggests that DBD1 is primarily responsible for initial DSB recognition and binding, thus facilitating DNA end resection and strand invasion in HR [7, 8, 9, 10, 11]. In contrast, DBD2 and BRCT preferentially bound G4 DNA, indicating a

focus on binding to non-canonical forms of DNA. The predicted locations of DBD1 and DBD2 on different, solvent-accessible surfaces of BRCA1 (Figure 6) support this separation of tasks, with DBD1 binding dsDNA and DBD2 targeting non-canonical DNA. As BRCT is situated within the interior of BRCA1 with less access to DNA, it correspondingly has lower binding affinities compared to the DBDs. However, DBD2 and BRCT may function together in binding non-canonical DNA due to their similar positioning on the left-most side of the model. A potential explanation for the difference in binding preferences is that the domains undergo structural changes when bound to DNA. DBD1 and DBD2 are primarily unstructured domains, while BRCT is composed of α helix and β sheets [50]. However, our CD studies (see Supporting Information) observed no significant conformational change when any of the domains bound to DNA. It is possible that the BRCA1 binding domain as a whole undergoes conformational changes upon DNA binding.

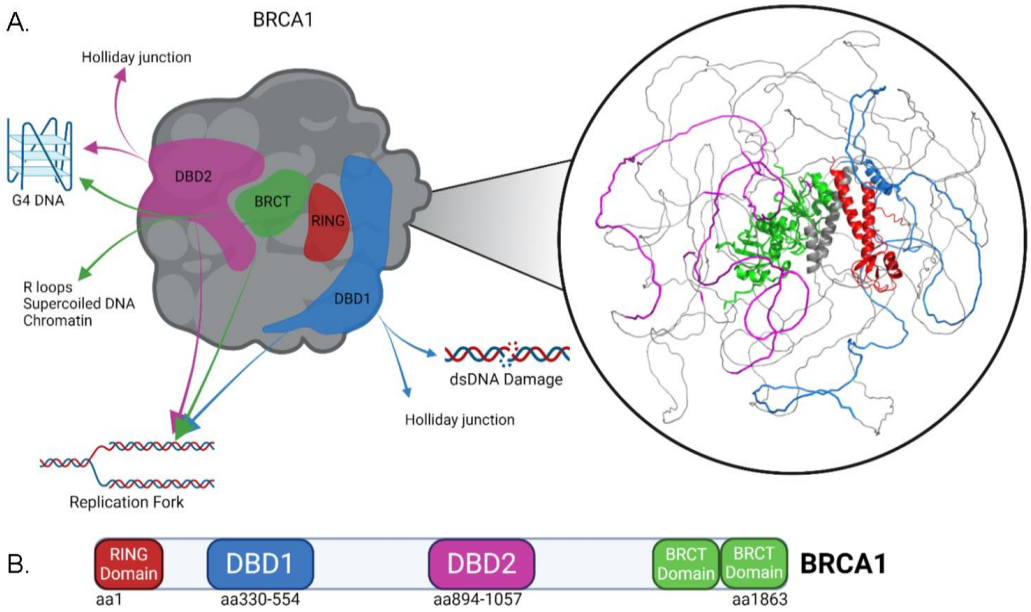

Figure 6. Models and map of BRCA1. **A.** Structural prediction of full-length BRCA1 using AlphaFold2 (right). Cartoon model (left) depicts the preferences of the different regions within BRCA1 in binding to distinct DNA structures. **B.** Cartoon map of BRCA1, highlighting domains RING (aa1-109, red), DBD1 (aa330-554, blue), DBD2 (aa894-1057, magenta), and the tandem BRCT repeats (aa1646-1863, green).

Sturdy et al. observed that aa230-534 preferentially bound to four-way junctions rather than to duplex and ssDNA, which does not align with our observations using the DBD1 construct [46]. However, DBD1 likely recognizes each arm of the cruciform structure as four separate double-stranded binding sites. It would be important to further validate the DNA binding affinities of DBD1 for each double-stranded binding site versus the overall binding affinity for the entire four-way junction. Conversely, Masuda et al. showed that aa421-701 prefers dsDNA over ssDNA [25]. Our DBD1 construct, which overlaps with residues 421-554, confirms these results. Next, we compared DBD2 to an aa444-1057 construct studied by Brázda et al. The study found that aa444-1057 bound strongest to non-canonical DNA such as quadruplex and cruciform DNA, rather than to dsDNA or ssDNA [26]. Our DBD2 construct retains this preference for non-canonical DNA. Although aa444-1057 overlaps part of DBD1, it contains the entirety of DBD2. Based on the Brázda et al. study, it appears that the DBDs can function together; however, it is likely that DBD2 is the driving force behind this binding preference for non-canonical DNA. Studies by Matsumoto et al. and Yamane et al. show the ability of BRCT to bind dsDNA and to recognize DNA breaks [43, 51]. We also demonstrate that BRCT binds to dsDNA. As our G4 sequence is present in human telomeric DNA, we support the model proposed by Hu et al. that BRCA1 BRCT remodels chromatin when tethered to chromosomes [41].

In summary, our experiments demonstrate that the DBD1, DBD2, and BRCT domains of BRCA1 have preferences for distinct DNA repair intermediates. Further studies of interactions between the entirety of the DBD (aa330-1057) and our three DNA repair intermediates should clarify whether the domain retains binding preferences that are more similar to DBD1 or to DBD2.

Materials and Methods

Buffers and reagents

All buffers and reagents were prepared with research grade chemicals and Type I water that was purified from a Smart2Pure 6 UV/UF system (ThermoFisher; Waltham, MA, USA). All solutions were sterilized through a 0.22 µm PES filter.

Expression and purification of recombinant proteins

E. coli constructs used to produce human BRCA1 DBD1 (aa330-554), DBD2 (aa894-1057), and BRCT (aa1646-1863) were purchased from VectorBuilder Inc. (Chicago, IL, USA). The plasmids were transformed into NiCo21(DE3) competent cells (New England Biolabs; Ipswich, MA, USA). For each construct, a 125 mL overnight starter culture was diluted (1:20) into 4 L of LB broth that was maintained at 37 °C and 250 rpm using a MaxQ 4000 orbital shaker (ThermoFisher). Protein expression was induced with 1 mM IPTG when the OD_{600} reached 0.6. Cells were harvested 4 hours post-induction by centrifugation using a J6-MI high-capacity centrifuge equipped with a JS-4.2 rotor (4,000 rpm at 4 °C for 90 minutes). The pellets were resuspended in 20 mM NaPi (pH 7.5), 300 mM NaCl, 30 mM imidazole, 1 mM DTT, 5% (v/v) glycerol, 1% NP-40, and 1 mM PMSF, and cells were lysed using a Fisherbrand 505 Dismembrator (Fisher Scientific; Hampton, NH, USA). Samples were chilled on ice during sonication (15 seconds on, 45 seconds off, and 45% amplitude for 15 minutes). Lysates were clarified by centrifugation with a Sorvall RC5C Plus high-speed centrifuge and a SS-34 fixed angle rotor (18,500 rpm at 4 °C for 90 minutes). The supernatant was filtered through a 0.45 µm PES membrane prior to liquid chromatography.

All protein purification steps were performed either on ice or in a 4 °C cold room. An Econo-Column (Bio-Rad; Hercules, CA, USA) filled with 20 mL Ni-NTA agarose (Goldbio; St. Louis, MO, USA) was equilibrated with 20 mM NaPi (pH 7.5), 300 mM NaCl, 30 mM imidazole, 1 mM DTT, and 5% glycerol. The filtered supernatant was mixed with the resin for 45 minutes to allow batch binding. The glass column was washed with 10 column volumes (CV) of equilibration buffer, followed by 10 CV of 20 mM NaPi (pH 7.5), 30 mM NaCl, 30 mM imidazole, 1 mM DTT, and 5% glycerol. The protein of interest was eluted with 1 CV of 20 mM NaPi (pH 7.5), 30 mM NaCl, 300 mM imidazole, 1 mM DTT, and 5% glycerol.

The Ni-NTA elution was immediately loaded onto a 5 mL HiTrap Heparin HP column (GE Healthcare, Chicago, IL, USA) that was equilibrated with 20 mM HEPES (pH 7.5), 30 mM NaCl, 5 mM TCEP, and 5% glycerol using an AKTA Start FPLC system (GE Healthcare). The column was washed with 10 CV of the equilibration buffer, and the protein was eluted with 20 mM HEPES (pH 7.5), 1 M NaCl, 5 mM TCEP, and 5% glycerol over a 50 mL linear gradient in 2 mL fractions. Fractions containing BRCA1 DBDs or BRCT were identified by SDS-PAGE, pooled, and dialyzed against storage buffer (20 mM HEPES pH 7.5, 150 mM KCl, 5 mM TCEP, and 20% glycerol) using 3500 MWCO tubing (ThermoFisher). After 3 dialysis exchanges, the protein was flash frozen in liquid nitrogen and stored at -80 °C until use. Protein concentrations were determined using a NanoDrop One C spectrophotometer (ThermoFisher) and molar extinction coefficients (Table 2).

Table 2. Peptide Sequences of BRCA1 DBD1, DBD2, and BRCT.

Name	**Sequence (N→C)**	**Molar Extinction Coefficient ($M^{-1}cm^{-1}$)**
6xHist-TEV-BRCT (aa1646-1863)	HHHHHHENLYFQGVNKRMSMVVSGLTPEEFMLV YKFARKHHITLTNLITEETTHVVMKTDAEFVCERT LKYFLGIAGGKWVVSYFWVTQSIKERKMLNEHD FEVRGDVVNGRNHQGPKRARESQDRKIFRGLEIC CYGPFTNMPTDQLEWMVQLCGASVVKELSSFTL GTGVHPIVVVQPDAWTEDNGFHAIGQMCEAPVV TREWVLDSVALYQCQELDTYLIPQIPHSHY	39,420
6xHist-TEV-DBD1 (aa330-554)	HHHHHHENLYFQGDRRTPSTEKKVDLNADPLCE RKEWNKQKLPCSENPRDTEDVPWITLNSSIQKVN EWFSRSDELLGSDDSHDGESESNAKVADVLDVLN EVDEYSGSSEKIDLLASDPHEALICKSERVHSKSV ESNIEDKIFGKTYRKKASLPNLSHVTENLIIGAFVT EPQIIQERPLTNKLKRKRRPTSGLHPEDFIKKADLA VQKTPEMINQGTNQTEQNGQVMNITNSGHE	20,970

6xHist-TEV-DBD2 (aa894-1057)	HHHHHHENLYFQGKQSPKVTFECEQKEENQGKNESNIKPVQTVNITAGFPVVGQKDKPVDNAKCSIKGGSRFCLSSQFRGNETGLITPNKHGLLQNPYRIPPLFPISFVKTKCKKNLLEEFEEHSMSPEREMGNENIPSTVSTISRNNIRENVFKEASSSNINEVGSSTNEVGSS	2,980

DNA oligos

DNA oligonucleotides were purchased from Integrated DNA Technologies (IDT; Coralville, IA, USA). Oligos were dissolved in Buffer H (20 mM HEPES pH 7.5, 150 mM KCl, 5 mM TCEP, and 5% glycerol), and DNA concentrations were measured using a NanoDrop One C spectrophotometer (ThermoFisher). Double-stranded DNA was prepared by mixing the non-biotinylated complementary strand in 1.05x molar excess over the biotinylated oligo, incubating the sample at 95 °C for 10 minutes, and cooling it slowly to room temperature over 6 hours.

Bio-layer interferometry (BLI)

BLI studies were performed on a BLItz instrument (Pall ForteBio, Fremont, CA, USA) in Buffer H at 25 °C. High precision streptavidin-coated biosensors (SA) were purchased from ForteBio and hydrated in Buffer H for 10 minutes prior to use. For each experiment, the sensor was placed in Buffer H for 30 seconds to collect an initial baseline. Next, 150 nM of biotinylated DNA was loaded onto the sensor over 120 seconds and a second baseline was collected in Buffer H for 30 seconds. Protein samples were then introduced at different concentrations. The association reactions were monitored for 180 seconds, and dissociation of the complexes were examined for 120 seconds in Buffer H. A reference curve was obtained in buffer alone and was subtracted from the other traces. BLI measurements were performed in triplicates on separate days.

Data analysis

BLI binding isotherms were generated by plotting the steady-state plateau values of the association phase against total analyte concentration. The curves were fit to a 1:1 interaction model by using Scientist 3.0 software (Micromath; St. Louis, MO) to solve the following implicit formulas, where Δλ was the observed signal change, A was the amplitude, and K was the equilibrium association constant. D_f and D_t were the free and total concentration of DNA, while P_f and P_t described the free and total concentration of the protein. The values reported were determined from the average and 95% confidence interval of three independent data sets.

$$\Delta\lambda = A\left(\frac{KP_f}{1 + KP_f}\right)$$
$$D_t = D_f\left(1 + KP_f\right)$$
$$P_t = P_f\left(1 + KD_f\right)$$

Acknowledgements

Figures 2 and 6 were created with BioRender.com.

Author contributions

CGW designed experiments. KL, LC, and CGW acquired data and interpreted results. KL, LC, EC, and CGW prepared the manuscript draft. All authors have read and agreed to the published version of the manuscript.

Funding and additional information

This work was supported by AHA grant 19AIREA34460026 to CGW.

Conflict of interest

Authors have no conflict of interest to disclose.

Data availability

All data are contained within the manuscript.

References

1. Wu, J.; Lu, L.-Y.; Yu, X., The role of BRCA1 in DNA damage response. *Protein Cell* **2010,** *1* (2), 117-123.
2. Rosen, E. M., BRCA1 in the DNA damage response and at telomeres. *Front. Genet.* **2013,** *4* (85).
3. Zhao, W.; Wiese, C.; Kwon, Y.; Hromas, R.; Sung, P., The BRCA Tumor Suppressor Network in Chromosome Damage Repair by Homologous Recombination. *Annu. Rev. Biochem.* **2019,** *88*, 221-245.
4. Ballal, R. D.; Saha, T.; Fan, S.; Haddad, B. R.; Rosen, E. M., BRCA1 Localization to the Telomere and Its Loss from the Telomere in Response to DNA Damage. *J. Biol. Chem.* **2009,** *284* (52), 36083-36098.
5. King, M.-C.; Marks, J. H.; Mandell, J. B.; New York Breast Cancer Study Group, Breast and Ovarian Cancer Risks Due to Inherited Mutations in BRCA1 and BRCA2. *Science* **2003,** *302* (5645), 643-646.
6. Nikfarjam, S.; Singh, K. K., DNA damage response signaling: A common link between cancer and cardiovascular diseases. *Cancer Med.* **2022,** *12* (4), 4380-4404.
7. Daley, J. M.; Sung, P., 53BP1, BRCA1, and the Choice between Recombination and End Joining at DNA Double-Strand Breaks. *Mol. Cell. Biol.* **2023,** *34* (8), 1380-1388.
8. Ceccaldi, R.; Rondinelli, B.; D'Andrea, A. D., Repair Pathway Choices and Consequences at the Double-Strand Break. *Trends Cell Biol.* **2016,** *26* (1), 52-64.
9. Sy, S. M. H.; Huen, M. S. Y.; Chen, J., PALB2 is an integral component of the BRCA complex required for homologous recombination repair. *Proc. Natl. Acad. Sci. U. S. A.* **2009,** *106* (17), 7155-7160.
10. Zhang, F.; Ma, J.; Wu, J.; Ye, L.; Cai, H.; Xia, B.; Xiaochun, Y., PALB2 Links BRCA1 and BRCA2 in the DNA-Damage Response. *Curr. Biol.* **2009,** *19* (6), 524-529.
11. Zhang, F.; Fan, Q.; Ren, K.; Andreassen, P. R., PALB2 Functionally Connects the Breast Cancer Susceptibility Proteins BRCA1 and BRCA2. *Mol. Cancer Res.* **2009,** *7* (7).
12. Chaudhuri, A. R.; Callen, E.; Ding, X.; Gogola, E.; Duarte, A. A.; Lee, J.-E.; Wong, N.; Lafarga, V.; Calvo, J. A.; Panzarino, N. J.; et al., Replication fork stability confers chemoresistance in BRCA-deficient cells. *Nature* **2016,** *535*, 382-387.
13. Xu, Y.; Ning, S.; Wei, Z.; Xu, R.; Xu, X.; Xing, M.; Guo, R.; Xu, D., 53BP1 and BRCA1 control pathway choice for stalled replication restart. *eLife* **2017,** *6*.
14. Zeman, M. K.; Cimprich, K. A., Causes and consequences of replication stress. *Nat. Cell Biol.* **2014,** *16* (1), 2-9.
15. Cortez, D., Preventing replication fork collapse to maintain genome integrity. *DNA Repair* **2015,** *32*, 149-157.
16. Li, M. L.; Greenberg, R. A., Links between genome integrity and BRCA1 tumor suppression. *Trends Biochem. Sci.* **2012,** *37* (10), 418-424.
17. Kass, E. M.; Moynahan, M. E.; Jasin, M., When Genome Maintenance Goes Badly Awry. *Mol. Cell* **2016,** *62* (5), 777-787.
18. Daley, J. M.; Niu, H.; Miller, A. S.; Sung, P., Biochemical mechanism of DSB end resection and its regulation. *DNA Repair* **2015,** *32*, 66-74.

19. Verma, P.; Greenberg, R. A., Noncanonical views of homology-directed DNA repair. *Genes Dev.* **2016,** *30* (10), 1138-1154.
20. Filippo, J. S.; Sung, P.; Klein, H., Mechanism of Eukaryotic Homologous Recombination. *Annu. Rev. Biochem.* **2008,** *77*, 229-257.
21. Rickman, K.; Smogorzewska, A., Advances in understanding DNA processing and protection at stalled replication forks. *J. Cell Biol.* **2019,** *218* (4), 1096-1107.
22. Bansal, A.; Kaushik, S.; Kukreti, S., Non-canonical DNA structures: Diversity and disease association. *Front. Genet.* **2022,** *13*.
23. Paull, T. T.; Cortez, D.; Bowers, B.; Elledge, S. J.; Gellert, M., Direct DNA binding by Brca1. *Proc. Natl. Acad. Sci. U. S. A.* **2001,** *98* (11), 6086-6091.
24. Zhao, W.; Steinfeld, J. B.; Liang, F.; Chen, X.; Maranon, D. G.; Ma, C. J.; Kwon, Y.; Rao, T.; Wang, W.; Sheng, C.; et al., BRCA1–BARD1 promotes RAD51-mediated homologous DNA pairing. *Nature* **2017,** *550*, 360-365.
25. Masuda, T.; Xu, X.; Dimitriadis, E. K.; Lahusen, T.; Deng, C.-X., "DNA Binding Region" of BRCA1 Affects Genetic Stability through modulating the Intra-S-Phase Checkpoint. *Int. J. Biol. Sci.* **2016,** *12* (2), 133-143.
26. Brázda, V.; Hároníková, L.; Liao, J. C. C.; Fridrichová, H.; Jagelská, E. B., Strong preference of BRCA1 protein to topologically constrained non-B DNA structures. *BMC Mol. Biol.* **2016,** *17* (14).
27. Zhu, Q.; Pao, G. M.; Huynh, A. M.; Suh, H.; Tonnu, N.; Nederlof, P. M.; Gage, F. H.; Verma, I. M., BRCA1 tumour suppression occurs via heterochromatin-mediated silencing. *Nature* **2011,** *477*, 179-184.
28. Zimmer, J.; Tacconi, E. M. C.; Folio, C.; Badie, S.; Porru, M.; Klare, K.; Tumiati, M.; Markkanen, E.; Halder, S.; Ryan, A.; et al., Targeting BRCA1 and BRCA2 Deficiencies with G-Quadruplex-Interacting Compounds. *Mol. Cell* **2016,** *61* (3), 449-460.
29. Xu, H.; Di Antonio, M..; McKinney, S.; Mathew, V.; Ho, B.; O'Neil, N. J.; Dos Santos, N.; Silvester, J.; Wei, V.; Garcia, J.; et al., CX-5461 is a DNA G-quadruplex stabilizer with selective lethality in BRCA1/2 deficient tumours. *Nat. Commun.* **2017,** *8*.
30. Wu, L. C.; Wang, Z. W.; Tsan, J. T.; Spillman, M. A.; Phung, A.; Xu, X. L.; Yang, M.-C. W.; Hwang, L.-Y.; Bowcok, A. M.; Baer, R., Identification of a RING protein that can interact in vivo with the BRCA1 gene product. *Nat. Genet.* **1996,** *14*, 430-440.
31. Hashizume, R.; Fukuda, M.; Maeda, I.; Nishikawa, H.; Oyake, D.; Yabuki, Y.; Ogata, H.; Ohta, T., The RING Heterodimer BRCA1-BARD1 Is a Ubiquitin Ligase Inactivated by a Breast Cancer-derived Mutation. *J. Biol. Chem.* **2001,** *276* (18).
32. Chen, A.; Kleiman, F. E.; Manley, J. L.; Ouchi, T.; Pan, Z.-Q., Autoubiquitination of the BRCA1·BARD1 RING Ubiquitin Ligase. *J. Biol. Chem.* **2002,** *277* (24), 22085-22092.
33. Tarsounas, M.; Sung, P., The antitumorigenic roles of BRCA1–BARD1 in DNA repair and replication. *Nat. Rev. Mol. Cell Biol.* **2020,** *21*, 284-299.
34. Bork, P.; Hofmann, K.; Bucher, P.; Neuwald, A. F.; Altschul, S. F.; Koonin, E. V., A superfamily of conserved domains in DNA damage-responsive cell cycle checkpoint proteins. *FASEB J.* **1997,** *11* (1), 68-76.
35. Botuyan, M. V. E.; Nominé, Y.; Yu, X.; Juranic, N.; Macura, S.; Chen, J.; Mer, G., Structural Basis of BACH1 Phosphopeptide Recognition by BRCA1 Tandem BRCT Domains. *Structure* **2004,** *12* (7), 1137-1146.

36. Clapperton, J. A.; Manke, I. A.; Lowery, D. M.; Ho, T.; Haire, L. F.; Yaffe, M. B.; Smerdon, S. J., Structure and mechanism of BRCA1 BRCT domain recognition of phosphorylated BACH1 with implications for cancer. *Nat. Struct. Mol. Biol.* **2004,** *11*, 512-518.
37. Shiozaki, E. N.; Gu, L.; Yan, N.; Shi, Y., Structure of the BRCT Repeats of BRCA1 Bound to a BACH1 Phosphopeptide: Implications for Signaling. *Mol. Cell* **2004,** *14* (3), 405-412.
38. Wu, C. G.; Spies, M., G-quadruplex recognition and remodeling by the FANCJ helicase *Nucleic Acids Res.* **2016,** *44* (18), 8742-8753.
39. Leung, C. C. Y.; Glover, J. N. M., BRCT domains: Easy as one, two, three. *Cell Cycle* **2011,** *10* (15), 2461-2470.
40. Rudolph, J.; Muthurajan, U. M.; Palacio, M.; Mahadevan, J.; Roberts, G.; Erbse, A. H.; Dyer, P. N.; Luger, K., The BRCT domain of PARP1 binds intact DNA and mediates intrastrand transfer. *Mol. Cell* **2021,** *81* (24), 4994-5006.e5.
41. Hu, Y.-F.; Hao, Z. L.; Li, R., Chromatin remodeling and activation of chromosomal DNA replication by an acidic transcriptional activation domain from BRCA1. *Genes Dev.* **1999,** *13* (6), 637-642.
42. Yamane, K.; Tsuruo, T., Conserved BRCT regions of TopBP1 and of the tumor suppressor BRCA1 bind strand breaks and termini of DNA. *Oncogene* **1999,** *18*, 5194-5203.
43. Chang, C.-W.; Singh, A. K.; Li, M.; Guan, L.; Le, N.; Omabe, K.; Liang, F.; Liu, Y., The BRCA1 BRCT promotes antisense RNA production and double-stranded RNA formation to suppress ribosomal R-loops. *Proc. Natl. Acad. Sci. U. S. A.* **2022,** *119* (50).
44. Mark, W.-Y.; Liao, J. C. C.; Lu, Y.; Ayed, A.; Laister, R.; Szymczyna, B.; Chakrabartty, A.; Arrowsmith, C. H., Characterization of Segments from the Central Region of BRCA1: An Intrinsically Disordered Scaffold for Multiple Protein–Protein and Protein–DNA Interactions? *J. Mol. Biol.* **2005,** *345* (2), 275-287.
45. Naseem, R.; Webb, M., Analysis of the DNA Binding Activity of BRCA1 and Its Modulation by the Tumour Suppressor p53. *PLoS One* **2008,** *3* (6).
46. Sturdy, A.; Naseem, R.; Webb, M., Purification and Characterisation of a Soluble N-terminal Fragment of the Breast Cancer Susceptibility Protein BRCA1. *J. Mol. Biol.* **2004,** *340* (3), 469-475.
47. Brázda, V.; Jagelska, E. B.; Liao, J. C. C.; Arrowsmith, C. H., The Central Region of BRCA1 Binds Preferentially to Supercoiled DNA. *J. Biomol. Struct. Dyn.* **2009,** *27* (1), 97-103.
48. Naseem, R.; Sturdy, A.; Finch, D.; Jowitt, T.; Webb, M., Mapping and conformational characterization of the DNA-binding region of the breast cancer susceptibility protein BRCA1 *Biochem. J.* **2006,** *395* (3), 529-535.
49. Peña-Guerrero, J.; Fernández-Rubio, C.; García-Sosa, A. T.; Nguewa, P. A., BRCT Domains: Structure, Functions, and Implications in Disease—New Therapeutic Targets for Innovative Drug Discovery against Infections. *Pharmaceutics* **2023,** *15* (7).
50. Williams, R. S.; Green, R.; Glover, J. N. M., Crystal structure of the BRCT repeat region from the breast cancer-associated protein BRCA1. *Nat. Struct. Biol.* **2001,** *8*, 838-842.
51. Matsumoto, T.; Go, K.; Hyodo, M.; Koiwai, K.; Maezawa, S.; Hayano, T.; Suzuki, M.; Koiwai, O., BRCT domain of DNA polymerase μ has DNA-binding activity and promotes the DNA polymerization activity. *Genes Cells* **2012,** *17* (9), 790-806.